Food Biophysics (2023) 18:488–496
https://doi.org/10.1007/s11483-023-09790-x

RESEARCH

Effect of *Curcuma longa* L. Extract and Curcumin on Porcine Pancreatic α–Amylase Structure and Activity

Grazielle Oliveira[1] · Elaine Kaspchak[1] · Anielle de Oliveira[2] · Fernanda Vitória Leimann[2,3] · Gisele Strieder Philippsen[4] · Flavio Augusto Vicente Seixas[5] · Luciana Igarashi-Mafra[1] · Marcos R. Mafra[1]

Received: 8 March 2022 / Accepted: 6 May 2023 / Published online: 23 May 2023

Abstract

This work aimed to evaluate α-amylase activity and structure in the presence of *Curcuma longa* L. extracts obtained with deep eutectic solvent (DES) and curcumin. Isothermal titration calorimetry (ITC), fluorescence, circular dichroism (CD), and molecular docking were applied to study the effect of additives on enzyme activity and structure. Results showed that in the presence of turmeric extracts, there was a lower catalytic rate. Through the ITC analysis, a lower reaction rate was noticed, related to the inhibition of the enzymatic activity, both in the presence of the extract and of curcumin. The turmeric extracts interacted with the enzyme by a static mechanism as demonstrated by fluorescence. CD showed an increase in negative bands characteristic of hydrophobic interactions between the enzyme and the samples, which probably difficult the access of substrate to the enzyme's active site. Molecular docking showed that curcumin is capable to interact with the active site of α-amylase confirming results obtained by other techniques. Results presented in this work show the turmeric extracts potential for α-amylase inhibition which may be of interest to the pharmaceutical and food industry.

Keywords Isothermal titration calorimetry · Fluorescence · Circular dichroism · Molecular Docking

Introduction

The α-amylases are enzymes that hydrolyze the α-(1,4) glycosidic bonds that constitute malto-oligosaccharides [1]. These enzymes are found in several plants, microbes, and animals [2], and have numerous applications in the food, textile, chemical, and paper industries [3, 4]. The porcine pancreatic α-amylase (PPA) is an endo-amylase and glycoprotein secreted of 55.4 kDa, presenting high efficiency in catalyzing the hydrolysis of α-(1,4) glycosidic bonds [5, 6].

In the human body, food starch is hydrolyzed into maltose, by the action of α-amylases [7] and subsequently converted into glucose by the action of alpha-glycosidases [8]. However, high levels of glucose in the blood can induce insulin deficiency, and deregulate glucose metabolism causing some chronic diseases such as hyperglycemia, diabetes, and cardiovascular diseases [9, 10]. Although there are already some commercial inhibitors of these enzymes, such as acarbose, migliol, and voglibose, these are associated with some adverse effects, so it the importance of finding viable alternatives, such as inhibitors from natural sources [11].

✉ Elaine Kaspchak
elaine.pe@ital.sp.gov.br

Grazielle Oliveira
grazielle@ufpr.br

1 Department of Chemical Engineering, Federal University of Paraná, Av. Francisco Heráclito dos Santos, n. 100, Curitiba, Paraná State PC 81531-980, Brazil

2 Post-Graduation Program of Food Technology (PPGTA), Federal University of Technology-Paraná, Campus Campo Mourão (UTFPR-CM), Via Rosalina Maria Dos Santos, 1233, Campo Mourão, Paraná CEP 87301-899, Brazil

3 Centro de Investigação de Montanha (CIMO), Instituto Politécnico de Bragança, Campus Santa Apolónia, Bragança 5300-253, Portugal

4 Federal University of Paraná, Campus Jandaia do Sul, Dr. Maximiano street, n. 426, Jandaia do Sul, Paraná CEP 86900-000, Brazil

5 Department of Technology, Universidade Estadual de Maringá, Av. Ângelo Moreira da Fonseca, 1800, Umuarama, PR CEP 87506-360, Brazil

Some natural compounds that can inhibit α-amylase activity are polyphenols [12–15], metal ions [16], and nanocrystalline cellulose [17]. Among the natural α-amylase inhibitors *Curcuma longa*, popularly called "turmeric", has great potential for application in the control of diabetes [18–20]. *Curcuma longa* is traditionally used in Indian cuisine and Ayurvedic medicine as a nutraceutical [19] and presents antioxidant, anti-inflammatory, antibacterial, anti-carcinogenic, and antiaging properties, mainly due to the action of curcumin, one of the agents responsible for the orange color and the aforementioned bioactive properties. [21]. The *Curcuma longa* extracts obtained using deep eutectic solvents (DES) show higher extraction of curcumin yield compared to conventional solvents, are not cytotoxic or genotoxic, and present several bioactivity properties [22].

To understand the effect and possible mechanisms of enzymatic inhibition, it is important to study the molecular interactions and the structural changes that occur in proteins. The α-amylase and its inhibitor interaction mechanisms can be evaluated by fluorescence spectroscopy [23]. Besides isothermal titration calorimetry (ITC) can be used to determine the kinetic constants of enzyme–substrate reactions by measuring the heat change that is proportional to the reaction rate [24]. Based on 3D structures, molecular docking can predict the conformation and probability of the binding between enzymes and ligands [25]. Given the above and trying to further explore the possible applications of DES-*curcuma* extracts in food products, the present study aims to evaluate the effect of curcumin, and *Curcuma longa* L. extracts on porcine pancreatic α-amylase structure and activity.

Materials and Methods

Materials

In this work *Curcuma longa* L., the rhizome was collected from specimens cultivated in Piraquara, Paraná State, Brazil (S 25° 503' 261″ and W 49° 003′ 917″). The reagents have the following specifications: menthol (Sigma-Aldrich - St. Louis, MO USA); lactic acid (Neon -São Paulo, SP, Brazil); acetic acid (Panreac - Barcelona, Spain); curcumin (Sigma-Aldrich – St. Louis USA); porcine pancreatic enzyme (Type VI-B, 10 units/mg solid, Sigma-Aldrich); potato starch (Sigma-Aldrich); sodium tartrate (Alphatec); sodium hydroxide (Isofar); dinitrosalicylic acid (Inlab); calcium chloride (Prochemicals) and sodium phosphate (Vetec).

Methods

Preparation of Deep Eutectic Solvents (DES) and Samples

The deep eutectic solvent (DES: menthol + lactic acid or Men:Lac), was prepared following the method described by Dai et al. [26]. The reagents were weighed on an analytical balance (Mettler Toledo model AL204) to achieve the 2:1 molar ratio of menthol to lactic acid. The mixtures were placed in a water bath with Dubnoff-type orbital agitation at a temperature of 70 °C for 4 h when a homogeneous and transparent liquid characteristic of DES can be noticed. The preparation of powders from rhizome from *Curcuma longa* L. and the selection of extraction conditions (1:20 sample to solvent mass ratio; 3 h; 45 °C) are described in our previous work [22]. The extractions were performed in an ultrasonic bath at 50 to 60 Hz (FS30D, Fisher Scientific Co.).

Isothermal Titration Calorimetry (ITC)

An isothermal titration calorimeter (ITC 200, Microcal Inc., Massachusetts, USA) was used to study the enzymatic kinetics of α-amylase from porcine pancreas according to the method described by Kaeswurm et al. [27] with some modifications. Protein samples were dialyzed against buffer (5 mM of phosphate buffer, pH 6.9, 15 mM of NaCl) overnight at 5 °C through a membrane of 12 kDa exclusion limit (St. Louis, Missouri, USA) and all solutions were prepared in the same dialysis buffer. After dialysis, the concentration of protein solutions was determined according to Bradford [28]. ITC measurements were conducted in a single injection experiment. Following an equilibration time of 10 min, 35 µL α-amylase in the concentration of 0.010 mg.mL^{-1} was added to 10 mg.mL^{-1} of the potato starch in the presence of Men:Lac extract (3.3×10^{-9} L/mL) or curcumin (33.5 µM). The temperature was maintained at 37 °C and the sample was stirred at 750 rpm. The resulting heat profile was transformed with the aid of Microcal Origin 7.0 software (ITC Data Analysis in Origin, MicroCal, LLC, Northampton, MA, U.S.A.) and the conversion rate was plotted against the substrate concentration [S]. The rate R_t of the substrate decomposition reaction is directly proportional to the power output in the calorimeter cell as described by Eq. (1).

$$R_t = \frac{P}{\Delta H \times V_0} \quad (1)$$

where P is the power generated by the reaction, ΔH is the heat of decomposition of the substrate and V_0 is the cell volume. The catalytic rate constant for substrate decomposition

(k_{cat}) and Michaelis constant (K_M) were calculated by Eq. (2).

$$R_t = \frac{k_{cat} \times [E]_{cat} \times [S]_t}{[S]_t + K_M} \quad (2)$$

where $[E]_{cat}$ is the total enzyme concentration and $[S]_t$ is the instantaneous concentration of the substrate.

Fluorescence

The spectra were recorded on a UV–Vis spectropolarimeter (J-815, Jasco International Co., Tokyo, Japan) coupled to a Peltier temperature controller (PTP-1). The protein concentration was 4 µM in the presence of curcumin (5.6 µM to 33.5 µM) or Men:Lac extract (0.6×10^{-3} to 3.3×10^{-3} µL per mL of solution). The excitation wavelength was set at 280 nm, and the emission signals were recorded from 300 to 450 nm. All experiments were performed at 37 °C. The appropriate control curves were subtracted from the sample curves. Quenching of α-amylase fluorescence was measured as described by the Stern–Volmer equation (Eq. 3).

$$\frac{F_0}{F} + k_q \tau_0 [Q] = 1 + K_{SV} [Q] \quad (3)$$

where F_0 and F are the fluorescence intensities before and after the addition of the quencher, respectively; k_q is the bimolecular quenching constant; τ_0 is the lifetime of the fluorophore in the absence of the quencher. [Q] is the concentration of the quencher, and K_{SV} is the Stern–Volmer quenching constant.

Circular Dichroism

The circular dichroism spectra were obtained using quartz cuvettes with an optical path of 0.1 and 1 cm width and were recorded from 190 to 300 nm using a J-815 CD spectropolarimeter (Jasco International Co). The protein concentration was 0.5 µM in the presence of curcumin (33.5 µM) or Men:Lac extract (0.6×10^{-3} µL per mL of solution). Nitrogen was used as the purge gas at a flow of 10 L min^{-1} and the experiments were performed at 37 °C in duplicate. Results were presented as molar mean residue ellipticity (θ_{MRE}) calculated by Eq. (4).

$$\theta_{\mathrm{MRE}} = \frac{(\theta - \theta_{control}) \times 100 \times M_{(M)}}{C \times l \times n} \quad (4)$$

where θ is the ellipticity degree (deg); $\theta_{control}$ is the ellipticity degree of the control sample (buffer or buffer + inhibitor); l is the optical length (cm); C is the concentration ($mg.mL^{-1}$); $M_{(M)}$ is the molar mass (kDa), and n is the number of protein residues. The θ_{MRE} is given in $deg.cm^2.dmol^{-1}$.

Molecular Docking

The tridimensional structure of the porcine pancreatic α-amylase (PDBid: 1HX0) modeled in the presence of ligand acarbose pentasaccharide (ARE) was prepared as described by Kato-Schwartz et al. [29]. The resulting modeled structure was used as the target for the docking simulations involving curcumin (CID 969,516), menthol (CID 1254), and lactate (CID 612) compounds.

Three programs were used in simulations: Autodock-v4.2.3 (Morris et al., 2009), Molegro-v6.0 [31], and Vina [30], where Autodock and Vina were implemented in the PyRx-0.9 graphical interface [32]. The redocking of the reference ligand ARE onto the modeled porcine pancreatic α-amylase complex was performed to validate the docking protocol for each program, where validation was confirmed when the best-ranked pose showed a root-mean-square deviation below 2.0 Å, in all repetitions. The search box for Autodock was centered at the reference ligand (grid dimension of *x*, *y*, and *z* equal to 50) and the parameters *number of runs* and *number of energy evaluations* were set to 50 and 2,500,000 respectively. Simulations in the Molegro were performed using a search radius of 11 Å centered in the reference ligand. The search algorithm Iterated Simplex and the scoring algorithm Moldock Score [grid] were applied, with 10 runs in each simulation. For Vina, the search box (dimensions of *x*, *y*, and *z* was set to 20, 15, and 20, respectively), centered in the reference ligand. Other parameters not mentioned for the three programs were set as default. At least, four repetitions were conducted for each program and the resulting average scores were analyzed. The relative score was calculated as proposed by Moreira and co-workers [33].

Statistical Analysis

The experimental data were presented as the mean ± standard deviation of the replicates. Mean values were evaluated by analysis of variances (ANOVA) followed by the Tukey test at 95% significance level with the aid of Statistica version 10.0 (StatSoft, Tulsa, Oklahoma, U.S.A.)

Results and Discussion

In our previous work [22], it was selected ideal solvents, temperatures, and time for the extraction of bioactive compounds present in the rhizome, leaf, and flower of *Curcuma longa* L. The extracts obtained an effect on porcine

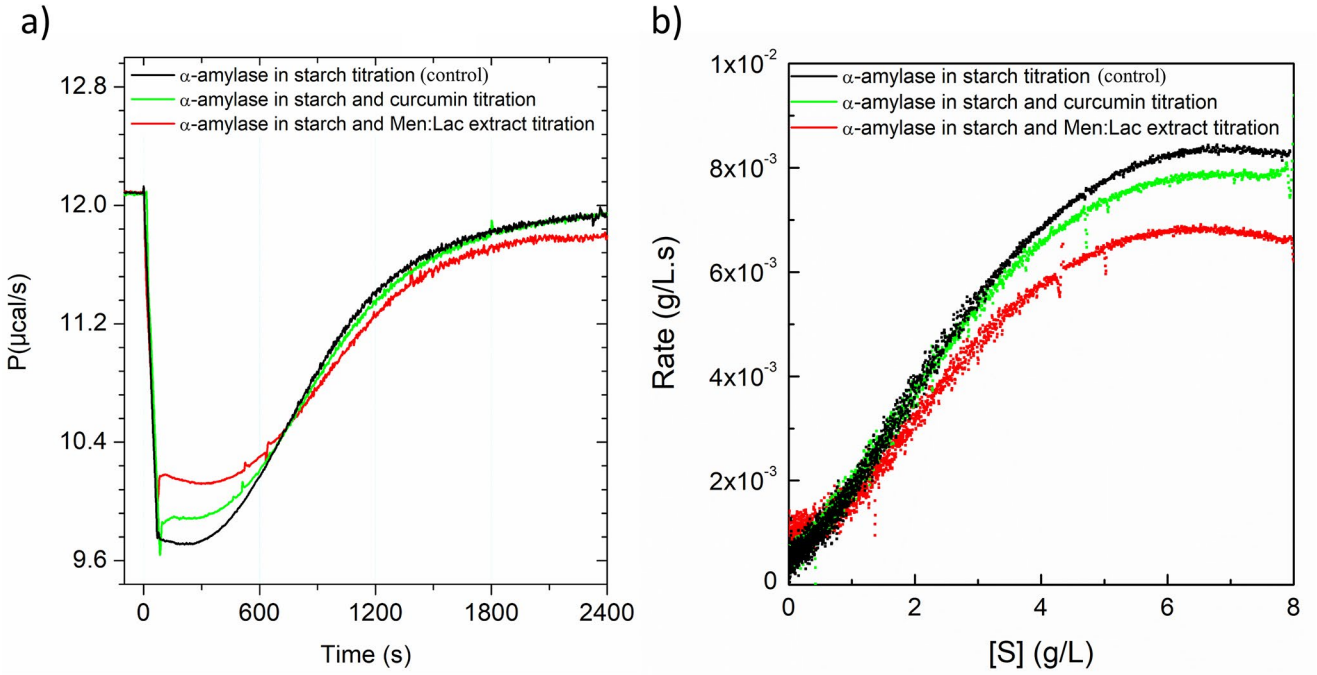

Fig. 1 Enzyme kinetics of starch hydrolysis by porcine α-amylase obtained by isothermal titration calorimetry. (**a**) ITC curve for potato starch conversion (200 µL; 10 mg/mL) after addition of porcine α-amylase (35 µL; 0.010 mg/mL). (**b**) Michaelis-Menten plot converted from ITC curve

pancreatic *α*-amylase enzyme activity was studied and the results are presented in Fig. S1 from Supplementary information. Based on the preliminary tests that indicated the turmeric extracts *α*-amylase inhibition capacity, the DES Men:Lac was used for the ITC, spectroscopic, and molecular docking experiments in optimized concentration due to the techniques and solubility limitations. The extract was chosen, considering possible applications in products intended for human consumption, since the results of previous biological analyzes showed a greater potential of inhibition for this sample, when compared to those containing the leaves or flowers of *Curcuma longa* L. [22] and do not present sensorial characteristic that could compromise product acceptance, due to the characteristic smell of acetic acid.

Isothermal Titration Calorimetry (ITC)

The components of turmeric are curcumin, demethoxycurcumin, and bisdemethoxycurcumin, and these are collectively known as curcuminoids. Of these compounds, curcumin is generally investigated by the scientific community for its wide range of bioactivity [21]. In this work, ITC was used to determine the enzymatic kinetics of potato starch hydrolysis by α-amylase. The effect of curcumin and extract (Men:Lac extract) on the enzymatic kinetics was obtained by the addition of these compounds in the sample cell of the ITC. Figure 1a shows the ITC curve obtained from porcine α-amylase injection in the potato starch solution, the substrate of this enzyme. It was observed that the peak intensity decreased in the presence of the inhibitor curcumin and Men:Lac extracts, indicating a smaller rate of reaction and consequently, a lower conversion of starch to reduced sugars. The control titrations of ITC experiments are shown in Fig. S2 (*see supplementary information*).

Table 1 Catalytic rate constant (k_{cat}), Michaelis constant (K_m) and heat of decomposition of the substrate (ΔH) for potato starch conversion by porcine α-amylase obtained by isothermal titration calorimetry

PARAMETER	CONTROL	CURCUMIN	Men:Lac EXTRACT
k_{cat} (s^{-1})	16.15 ± 0.35^{a}	15.45 ± 0.07^{ab}	13.65 ± 0.35^{b}
k_m (mg/mL)	6.83 ± 0.16^{a}	5.93 ± 0.14^{a}	4.80 ± 0.88^{a}
ΔH (cal/mg)	-1407.50 ± 2.12^{a}	-1300 ± 117.38^{a}	-1392.50 ± 58.69^{a}

The averages followed by the same letters do not differ in the line at a 95% confidence level, according to the Tukey test

Some kinetic parameters of enzymatic reaction are relevant, such as the catalytic constant (k_{cat}) for the substrate-to-product conversion, and the Michaelis constant (K_m), which is defined as the substrate concentration needed, at the initial rate, to reach half of the maximum reaction speed. These parameters help to better understand the interaction between enzyme and substrate, and whether enzymes continue their activity [34]. Table 1 shows the values obtained by ITC data presented in Fig. 1b for K_{cat} and K_m, in the interaction reaction between α-amylase and the control, curcumin, and Men:Lac extract can be observed. In addition, the values of heat of decomposition of the substrate (ΔH) are presented.

Regarding the constant K_m, it is observed that there was no significant difference between treatments, demonstrating that both pure curcumin and the extract acted as non-competitive inhibitors [35]. Regarding the catalytic constant (k_{cat}), the order in converting moles of substrates into products also followed the K_m pattern, that is, the values of control > curcumin > Men:Lac extract. As all ΔH values found are negative, cf. Table 1, the enthalpy of the reactants is higher than those of the product, indicating that the reactions are exothermic, and the higher inhibition was observed in the presence of Men:Lac extract.

Fluorescence

Fluorescence is a technique widely used to study and analyze interactions between ligands and proteins. Changes in fluorescence intensity can occur due to many factors, such as excited state reactions, molecular rearrangements, formation of ground state complex, and due to energy transfer [36]. The fluorescence was used to evaluate the effects of curcumin and Men:Lac extracts on the porcine pancreatic α-amylase structure. When the protein is excited at 280 nm, it emits a fluorescence peak at 331 nm that is related to the presence of tryptophan residues protein. As shown in Fig. 2a and c, the fluorescence intensities of α-amylase displayed dose-dependent quenching with increasing amounts of curcumin and Men:Lac extract. The fluorescence spectra of the buffer are shown in Fig. S3 (*see supplementary information*). As the concentration of curcumin and Men:Lac extract increases the fluorescence intensity decreases. This is due to changes in the environment in the vicinity of the

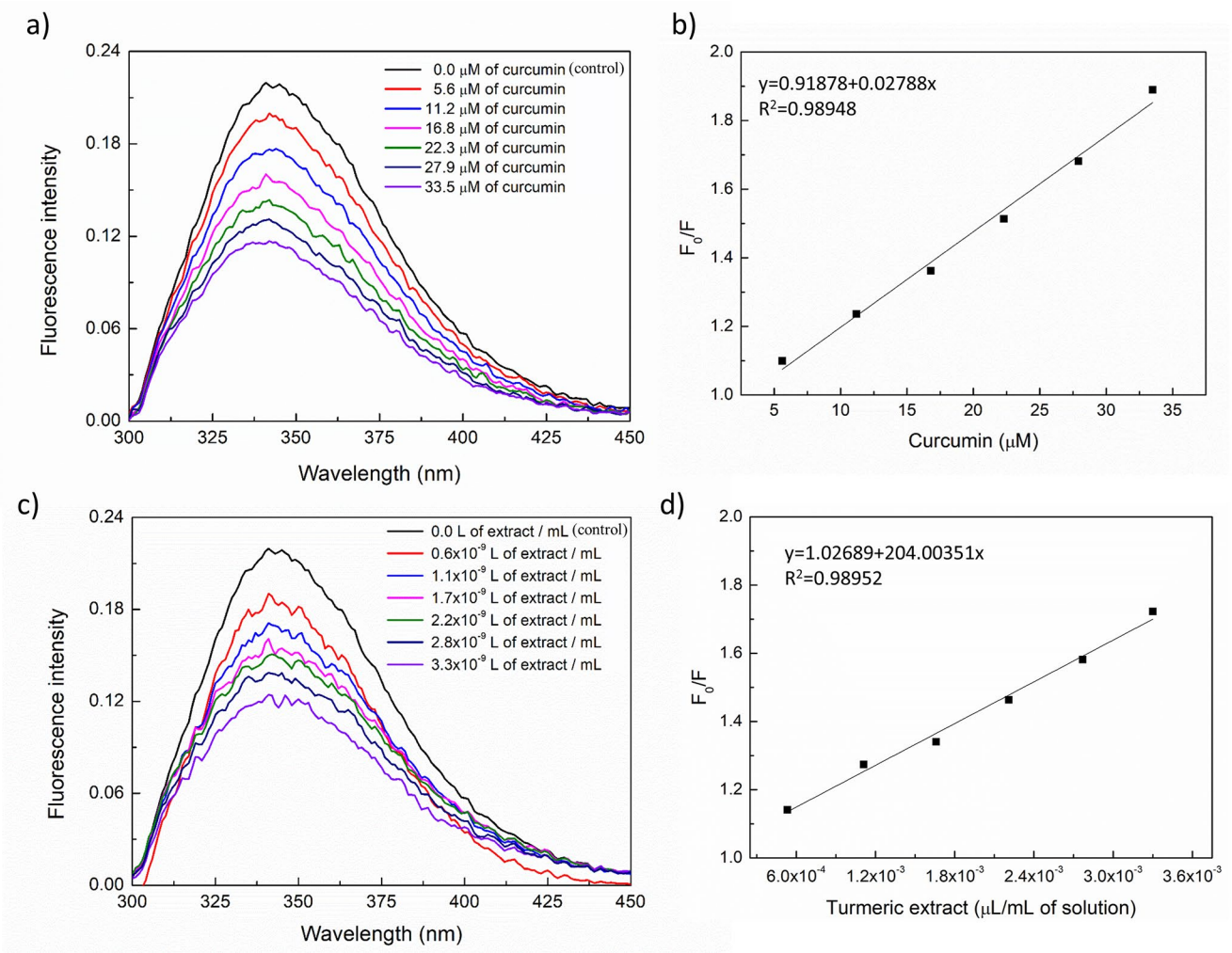

Fig. 2 Fluorescence experiments evaluating the impact of curcumin and Men:Lac extract on the tertiary structure of porcine α-amylase solutions (4 mM). (**a**) Emission spectra obtained in the presence of curcumin at concentrations ranging from 5.6 μM to 33.5 μM. (**b**) Stern–Volmer plot describing the quenching caused by curcumin. (**c**) Emission spectra obtained in the presence Men:Lac extract at concentration ranging from 0.6×10^{-9} to 3.3×10^{-9} L per mL of solution. (**d**) Stern–Volmer plot describing the quenching caused by Men:Lac extract. Fluorescence emissions intensity were recorded at 280 nm, and the maximum emission occurred at 341 nm

chromophore molecule due to protein and ligand interaction decreasing the fluorescence signal on the spectrum [37].

Figure 2b and d show the Stern–Volmer plots for curcumin and Men:Lac extract, respectively. It was observed a linear correlation between the quenching concentration and maximum fluorescence indicated one type of quenching mechanism [38]. The average fluorescence lifetime (τ_0) is approximately 10^{-9} s for α-amylase and quenching constants (k_q) higher than 10^{10} $M^{-1}.s^{-1}$ are attributed to a static mechanism [39]. In the present work, the k_q obtained was 9.39×10^{12} $M^{-1}.s^{-1}$ and 6.87×10^{13} $M^{-1}.s^{-1}$, for curcumin and Men:Lac extract, respectively, showing a static mechanism of interaction. This kind of quenching results from a non-fluorescent ground-state complex due to the insufficient energy of the quencher to collide with the excited state fluorophore [40]. These results show that both curcumin and Men:Lac extract compounds can interact with the enzyme resulting in the enzymatic activity decrease described in topic 3.1.

Circular Dichroism (CD)

The CD is a method that helps to explore and visualize changes in the secondary structure of peptides and proteins, in the presence of a given compound, with a comparison of its spectrum when there is no presence of these compounds [41]. Figure 3 shows the results of the CD spectra for the control, pure α-amylase, with curcumin and Men:Lac extract. The CD spectra of the buffer are shown in Fig. S4 (*see supplementary information*).

From the characteristic spectrum of porcine pancreatic α-amylase, control black curve cf. Figure 3, two negative bands between 208 and 225 nm are observed, with results similar to those obtained by Zheng et al. (2020). These bands are formed by $\pi \rightarrow \pi^*$ and $n \rightarrow \pi^*$ transitions of amide groups, which are typical features of α-helices conformations [42]. In the presence of curcumin, red curve cf. Figure 3, there was an increase in the intensity of these negative bands. This fact is attributed to the hydrophobic interactions between curcumin and the enzyme, and the α-helices content may have increased with the increase in the hydrophobicity of the medium [43], this fact may have happened with the extract. In the work developed by Zheng and coworkers (2020), the authors noticed that, through covalent bonds between the phenolic acid and the amino groups of the porcine pancreatic α-amylase, there was an increase in the content of the α -helices from 4.9 to 6.9%. The increase in hydrophobicity is related to hydrogen bonds, which alter the secondary structure of a-amylase, and hydrogen networks hinder the interaction channel between the enzyme's catalytic site and the substrate, leading to reduced enzyme activity [44].

Molecular Docking

Acarbose is a modified oligosaccharide that has an N group in place of the O of one of its glycosidic bonds (PubChem CID: 447,014). Since it is an inhibitor of α-glycosidases, which are involved in the degradation of disaccharides, oligosaccharides, and polysaccharides, acarbose exerts its

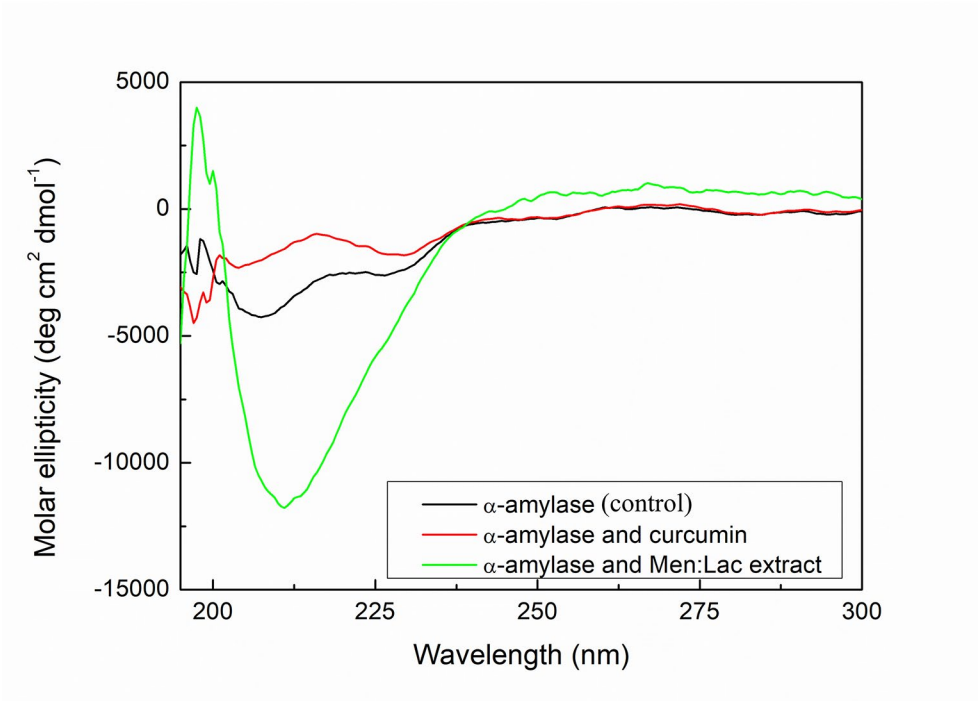

Fig. 3 UV circular dichroism spectrum of porcine α-amylase in the presence of 33.5μM of curcumin and 0.6×10^{-3} μL/mL of Men:Lac extract

Table 2 Average scores for evaluated compounds in the docking simulations considering the porcine pancreatic α-amylase as the target

Compounds	Autodock score	Molegro score	Vina score	Relative score
Acarbose pentasaccharide (ARE)	-5.96 ± 0.40	-177.44 ± 6.86	-9.0 ± 0.0	0.917
Curcumin (CID 969,516)	-7.93 ± 0.15	-119.95 ± 0.62	-8.3 ± 0.1	0.867
Menthol (CID 1254)	-5.33 ± 0.00	-54.07 ± 0.05	-5.9 ± 0.0	0.544
Lactate (CID 612)	-1.96 ± 0.03	-45.22 ± 0.07	-3.4 ± 0.1	0.293

activity in the intestinal tract and, therefore, causes adverse effects such as flatulence, diarrhea, and abdominal pain [45]. However, this mechanism is very efficient in decreasing blood glucose, which makes the inhibition of intestinal α-glucosidases an interesting target for new antihyperglycemic drugs [46]. Thus, it is justified to compare new candidates for α-amylase inhibitors with acarbose.

Table 2 summarizes the scores of the docking simulations of the compounds evaluated, regarding acarbose. None of the compounds investigated in this work presented a better relative score regarding acarbose, which means less probability of binding to porcine pancreatic α-amylase than acarbose. However, among them, curcumin was the one with the best relative score and, therefore, the highest probability of binding α-amylase about the others. This fact does not mean that the ligands evaluated do not bind to porcine pancreatic α-amylase; in fact, it only indicates a low probability of the compounds binding to the target enzyme and, therefore, the need for higher concentrations to bind and inhibit the enzyme activity.

Figure 4c shows the best pose of the curcumin obtained by each of the docking programs used. The fact that all the programs find similar poses suggests a binding pattern, which is typical for real inhibitors.

Figure 4a shows the best poses of curcumin found by the Molegro program from three simulations indicating a docking pattern. Figure 4b shows the interactions that curcumin makes with residues of the active site of porcine pancreatic α-amylase. On the other hand, Fig. 4d-e, shows the cluster of superimposed poses of the menthol and lactic acid found with the Molegro program. The fact that the program found several identical poses, which can be seen by the almost-perfect overlap, also suggests a binding pattern. However, due to their smaller size compared to canonical α-amylase ligands, such as starch or acarbose, these two ligands can be positioned elsewhere in the active site when evaluated by another program, which is not a typical behavior of a true ligand.

Although docking simulations cannot be interpreted as empirical evidence, they indicate a possible binding mechanism and highlight the ligands most likely to bind from a given library. In this regard, the results obtained by docking are following the results observed by the enzyme inhibition assays, where curcumin was the ligand with the greatest inhibition capacity.

Conclusion

The effect of curcumin and Men:Lac extract on α-amylase activity and structure was studied using isothermal titration calorimetry, fluorescence, circular dichroism, and molecular docking. Through the ITC analysis, it was possible to observe that in the presence of curcumin and Men:Lac extract, there was a lower reaction rate, related to the

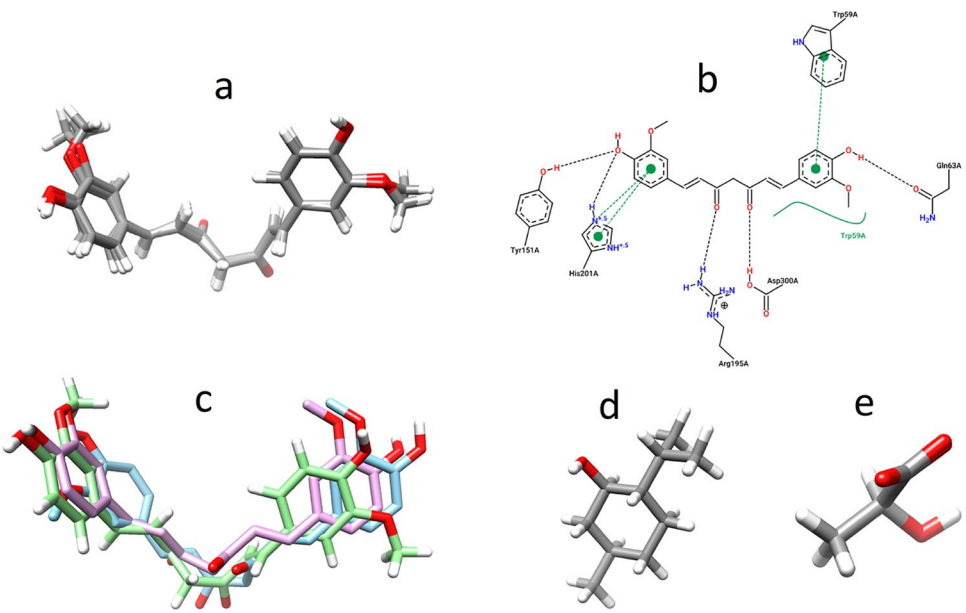

Fig. 4 Curcumin docked on the active site of porcine pancreatic α-amylase, showing a **c**luster of poses obtained from Molegro program (**A**) and the respective 2D interaction diagram (**B**) generated by the PoseView program [47]. (**C**) Pose of curcumin docked on the active site of porcine pancreatic α-amylase obtained in Autodock (blue), Molegro (green) and Vina (purple). Cluster of the poses with best scores obtained by Molegro for menthol (**D**) and lactate (**E**)

inhibition of enzymatic activity. The inhibition probably occur by noncompetitive inhibition since no significative difference was obtained for the Michalis constant. The turmeric extract and curcumin can interact with the enzyme by a static mechanism, as observed by fluorescence spectroscopy, and modification of the protein's secondary structure. Molecular docking indicated that curcumin is the compound most likely to bind to the active site of porcine pancreatic α-amylase compared to menthol and lactic acid. Results obtained by this work show that the curcumin and *Curcuma longa* extracts obtained by DES have a great potential to be used as potential α-amylase inhibitors and could be applied by the pharmaceutical and food industry to inhibit starch hydrolysis in the human body.

Supplementary Information The online version contains supplementary material available at https://doi.org/10.1007/s11483-023-09790-x.

Acknowledgements This study was financed by the Coordenação de Aperfeiçoamento de Pessoal de Nível Superior - Brazil (CAPES) – Finance Code 001. E. Kaspchak, M. R. Mafra, and L. Igarashi-Mafra are grateful to the Brazilian National Council for Scientific and Technological Development (CNPq - Grant 150906/2020-0, 310182/2018-2 and 308517/2018-0, respectively), and F. V. Leimann (CNPq - Grant 421541/2018-0). Fundação Araucária (40/2016 and 39/2019) and CENAPAD/SP (proj. 520).

Declarations

Competing interests The authors declare that they have no known competing financial interests or personal relationships that could have appeared to influence the work reported in this paper.

References

1. S. Janecek, Eur. J. Biochem. **224**, 519 (1994)
2. G. Muralikrishna, M. Nirmala, Carbohydr. Polym. **60**, 163 (2005)
3. R. Gupta, P. Gigras, H. Mohapatra, V.K. Goswami, B. Chauhan, Process. Biochem. **38**, 1599 (2003)
4. R. W. et al. Barbosa-Cánovas, G.; Davidson, P.M.; Dreher, M.; Hartel, Carbohydrates in Food, Second Edi (CRC Press, USA, 2006)
5. G. Prodanov, E.; Seigner, C.; Marchis-Mouren, Biochem. Biophys. Reserach Commun. **1**, 75 (1984)
6. S. Darnis, N. Juge, X.J. Guo, G. Marchis-Mouren, A. Puigserver, J.C. Chaix, Biochim. Biophys. Acta - Protein Struct. Mol. Enzymol. **1430**, 281 (1999)
7. A. Hess, S. Kress, S. Rakete, G. Muench, J. Kornhuber, M. Pischetsrieder, C.P. Müller, Behav. Brain Res. **364**, 328 (2019)
8. A.M. Dirir, M. Daou, A.F. Yousef, L.F. Yousef, *A Review of Alpha-Glucosidase Inhibitors from Plants as Potential Candidates for the Treatment of Type-2 Diabetes* (Springer Netherlands, 2021)
9. A.G. D'Amico, G. Maugeri, D. Rasà, C. Federico, S. Saccone, F. Lazzara, A. Fidilio, F. Drago, C. Bucolo, V. D'Agata, J. Cell. Physiol. **234**, 5230 (2019)
10. J.G. Knudsen, A. Hamilton, R. Ramracheya, A.I. Tarasov, M. Brereton, E. Haythorne, M.V. Chibalina, P. Spégel, H. Mulder, Q. Zhang, F.M. Ashcroft, J. Adam, P. Rorsman, Cell. Metab. **29**, 430 (2019)
11. H. Dehghan, P. Salehi, M.S. Amiri, Ind. Crops Prod. **117**, 303 (2018)
12. S. Liu, J. Yu, S. Guo, H. Fang, X. Chang, LWT - Food Sci. Technol **126**, 109288 (2020)
13. J.A.H.H. Kaeswurm, B. Claasen, M.P. Fischer, M. Buchweitz, J. Agric. Food Chem. **67**, 11108 (2019)
14. L. Sun, M.J. Gidley, F.J.F.J. Warren, Mol. Nutr. Food Res. **61**, 1700324 (2017)
15. L. Sun, F.J. Warren, M.J. Gidley, Y. Guo, M. Miao, Food Chem. **283**, 468 (2019)
16. M.U. Dahot, A.A. Saboury, A.A. Moosavi-Movahedi, J. Enzym Inhib. Med. Chem. **19**, 157 (2004)
17. J. Nsor-Atindana, H.D. Goff, M.N. Saqib, M. Chen, W. Liu, J. Ma, F. Zhong, Food Hydrocoll. **90**, 341 (2019)
18. M.A. Butala, S.K. Kukkupuni, P. Venkatasubramanian, C.N. Vishnuprasad, Starch/Staerke **70**, 1700182 (2018)
19. S. Ramkumar, H.V. Thulasiram, A. RaviKumar, J. Food Biochem. **45**, 1 (2021)
20. M. Najafian, Zahedan J. Res. Med. Sci. In Press, (2015)
21. J.P. Sahoo, L. Behera, J. Praveena, S. Sawant, A. Mishra, S.S. Sharma, L. Ghosh, A.P. Mishra, A.R. Sahoo, P. Pradhan, S. Sahu, A. Moharana, K.C. Samal, Am. J. Plant. Sci. **12**, 455 (2021)
22. G. Oliveira, C. Marques, A. de Oliveira, A. de Almeida dos W. Santos do R.P. Amaral, F.V. Ineu, A.P. Leimann, L. Peron, Igarashi-Mafra, M.R. Mafra, Innov. Food Sci. Emerg. Technol. 70, (2021)
23. R. Karoui, C. Blecker, Food Bioprocess. Technol. **4**, 364 (2011)
24. G. Lehoczki, K. Szabó, I. Takács, L. Kandra, G. Gyémánt, J. Enzyme Inhib. Med. Chem. **31**, 1648 (2016)
25. K. Crampon, A. Giorkallos, M. Deldossi, S. Baud, L. Angelo, Steffenel, Drug Discov. Today xxx, (2021)
26. Y. Dai, J. Van Spronsen, G.J. Witkamp, R. Verpoorte, Y.H. Choi, J. Van Spronsen, G.J. Witkamp, Anal. Chim. Acta **766**, 61 (2013)
27. J.A.H. Kaeswurm, L. Könighofer, M. Hogg, A. Scharinger, M. Buchweitz, Foods **9**, 367 (2020)
28. M.M. Bradford, Anal. Biochem. **72**, 248 (1976)
29. C.G. Kato-Schwartz, R.C.G. Corrêa, D. de Souza Lima, A.B. de Sá-Nakanishi, G. de Almeida Gonçalves, F.A.V. Seixas, C.W.I. Haminiuk, L. Barros, I.C.F.R. Ferreira, A. Bracht, R.M. Peralta, Food Res. Int. **137**, 109462 (2020)
30. A.J. Trott, O.; Olson, A.J. Morris, M. Garrett, R. Huey, W. Lindstrom, M.F. Sanner, R.K. Belew, D.S. Goodsell, Olson, J. Comput. Chem. **32**, 174 (2009)
31. M.H. Thomsen, R.; Christensen, J. Med. Chem. **49**, 3315 (2006)
32. S. Dallakyan, A. Olson, Glob. Food Secur. Gov **1263**, 1 (2015)
33. T.F.M. Moreira, L.G.A. Pessoa, F.A.V. Seixas, R.P. Ineu, O.H. Gonçalves, F.V. Leimann, R.P. Ribeiro, Food Chem. 367, (2022)
34. R. Eisenthal, M.J. Danson, D.W. Hough, Trends Biotechnol. **25**, 247 (2007)
35. M.H. Rodriguez, G. Jon-Marc, Towns, Chem. Educ. Res. Pract. 1 (2019)
36. M. Huang, R.C. Smart, C. Wong, A.H. Conney, Am. Assoc. Cancer **48**, 5941 (1988)
37. C.T.M. Kayukawa, M.A.S. de Oliveira, E. Kaspchak, H.B.S. Sanchuki, L. Igarashi-Mafra, M.R. Mafra, Food Chem. **275**, 346 (2019)
38. A. Papadopoulou, R.a. Frazier, Trends Food Sci. Technol **15**, 186 (2004)
39. X. Cai, J. Yu, L. Xu, R. Liu, J. Yang, Food Chem. **174**, 291 (2015)
40. L. Mátyus, J. Szöllosi, A. Jenei, J. Photochem. Photobiol B Biol. **83**, 223 (2006)
41. Y. Zheng, W. Yang, W. Sun, S. Chen, D. Liu, J. Funct. Foods **64**, 103587 (2020)

42. C.F. Rigos, D.L. Santos, G. Thedei, R.J. Ward, P. Ciancaglini, Int. Union Biochem. Mol. Biol. **31**, 329 (2003)
43. H. Ding, X. Wu, J. Pan, X. Hu, D. Gong, G. Zhang, J. Agric. Food Chem. **66**, 7065 (2018)
44. W. Xu, Y.; Xie, L.; Xie, J.; Liu, Yu; Chen, Chem. Commun. **55**, 39 (2019)
45. T. Fujisawa, H. Ikegami, K. Inoue, Y. Kawabata, T. Ogihara, Metabolism **54**, 387 (2005)
46. C.G. Kato, G. De Almeida Gonçalves, R.A. Peralta, F.A.V. Seixas, A.B. De Sá-Nakanishi, L. Bracht, J.F. Comar, A. Bracht, R.M. Peralta, Enzyme Res. 1 (2017)
47. K. Stierand, P.C. Maaß, M. Rarey, Bioinformatics **22**, 1710 (2006)